Lab-on-a-Bubble: Synthesis, Characterization, and Evaluation of Buoyant Gold Nanoparticle-Coated Silica Spheres

Virginia L. Schmit,[†] Richard Martoglio,[‡] Brandon Scott,[†] Aaron D. Strickland,[§] and Keith T. Carron[*,†,||]

[†]Chemistry Department, University of Wyoming, 1000 East University Avenue, Laramie, Wyoming 82071, United States

[‡]Department of Chemistry and Biochemistry, DePauw University, 602 South College Avenue, Greencastle, Indiana 46135, United States

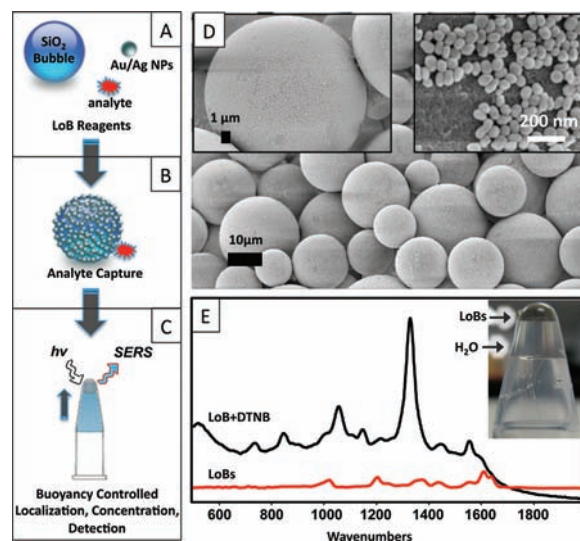[§]iFyber LLC, 950 Danby Road, Suite 300, Ithaca, New York 14850, United States

[||]Snowy Range Instruments, 628 Plaza Lane, Laramie, Wyoming 82070, United States

S *Supporting Information*

ABSTRACT: This paper describes the development and preparation of a new class of materials for surface-enhanced Raman scattering (SERS) consisting of gold nanoparticles coated onto hollow, buoyant silica microspheres. These materials allow for a new type of molecular assay designated as a lab-on-a-bubble (LoB). LoB materials serve as a convenient platform for the detection of analytes in solution and offer several advantages over traditional colloidal gold and planar SERS substrates, such as the ability to localize and concentrate analytes for detection. An example assay is presented using the LoB method and cyanide detection. Cyanide binds to SERS-active, gold-coated LoBs and is detected directly from the corresponding SERS signal. The abilities of LoBs and a gold colloid to detect cyanide are compared, and in both cases, a detection limit of ∼170 ppt was determined. Differences in measurement error using LoBs versus gold colloid are also described, as well as an assay for 5,5′-dithiobis(2-nitrobenzoic acid) that shows the benefit of using LoBs over SERS analyses in colloids, which are often plagued by particle aggregation.

Figure 1. (A−C) The basic components of a lab-on-a-bubble (LoB) assay for SERS-based detection of a analyte. (D) Representative SEM images of SERS-active AuNP-coated LoBs. (E) Representative Raman spectra of "naked" LoBs and LoBs in the presence of DTNB. The inset shows a picture of SERS-active buoyant LoBs in a microcentrifuge tube.

Micro- and nanoelectromechanical systems (MEMS and NEMS) have made significant impacts on chemical sensors. For example, the technology behind lab-on-a-chip (LOC) has emerged into a large market defining point-of-care (POC) diagnostics.[1] These novel systems represent combinations of miniaturized chemical separation methods and a variety of detection schemes. The drive toward miniaturized instrumentation and straightforward single-step assays has brought about the growth of these research efforts. One example of a nanopowered engine is the use of paramagnetic materials for separation and analyte capture. Paramagnetic engines are powered by external magnets that concentrate the assay results into a small, localized volume for more sensitive analysis. This scheme works well in small sample volumes and with sufficient time for exponentially decaying magnetic fields to impel the majority of the particles. In this article, we present a different method of nanopropulsion: buoyancy from a hollow silica "bubble" to produce a lab-on-a-bubble (LoB) (Figure 1).

Our initial work with paramagnetic nanoparticles was driven by a fundamental limitation to surface enhanced raman scattering (SERS) analysis with colloidal nanoparticles. This limitation originates with dispersive Raman instruments and the property of étendue. Succinctly, étendue describes the inverse relationship between spectral resolution and a spectrometer's optical throughput. In sampling of a nanoparticle solution, étendue coupled with a reasonable spectral resolution requires a focused beam from the excitation laser. Likewise, the colloidal nature of nanoparticles in solution requires that they be continually propelled by Brownian motion, and thus, individual particles move into and out of the focused laser beam. It is often desirable to use a small quantity of nanoparticles to maximize the surface coverage of a strongly adsorbing analyte; this leads to fluctuations in the SERS signal due to the Brownian motion-induced fluctuation of particles within the focal volume. Chemical analysis of the analyte concentration is limited by these fluctuations. It is desirable to have the noise in an experiment be limited by the shot noise of the detector, but as we will report, the noise in our colloidal nanoparticle experiments far exceeds the detector's shot noise.

SERS-active nanoparticles provide valuable information about species in aqueous media. However, their widespread use is limited by their instability. Recently, Pierre et al.[2] have shown the effect of nanoparticle instability on Au nanoparticle (AuNP) assays. They demonstrated the loss of signal due to changes in the AuNP surface as a result of adsorption of a neutral thiol species. Aggregation is also caused by changes in pH, ionic strength, and mixing parameters. The limitations of signal noise in excess of the detection system and the instability of nanoparticles under adsorptive processes are critical problems for viable SERS diagnostics.

In this study, we report results from a different approach to solution-phase analysis with SERS-active nanoparticles in which the separation mechanism is directly coupled to the detection method. The LoB concept is centered on a low-density particle that utilizes buoyant force to drive assay separation, while AuNPs coupled to the buoyant particles act as SERS nanosensors. Addition of a selective coating on the AuNPs creates the potential for smart sensors. In the current study, we report the detection of the generic thiol-containing Raman-active small molecule 5,5'-dithiobis(2-nitrobenzoic acid) (DTNB) as well as detection of cyanide, which is a relevant model analyte in environmental testing.

Figure 1 illustrates the concept of a direct LoB assay along with representative scanning electron micrographs and Raman data acquired from LoB reagents. In a typical LoB assay, the LoB reagents, buoyant SiO$_2$ bubbles and AuMPs or AgNPs, are combined to provide a SERS-active particle platform (Figure 1A,B) for the detection of target analytes by localizing them close to the bubble−NP composite (Figure 1B,C). Bubble flotation then drives the complex to a specified point in a reaction vessel where the analyte is selectively detected as a purified, concentrated LoB complex, as illustrated in Figure 1C. For the current study, AuNP-coated LoBs were prepared by first activating buoyant silica bubbles (3M Corporation) with aminopropyltriethoxysilane (APTES) following a standard protocol for glass (Figure 1A,B).[3,4] Colloidal gold was then incubated with the bubbles, resulting in controlled AuNP aggregation onto the bubble surface (Figure 1B,D); aggregates of AuNPs and AgNPs are known to exhibit strong enhancements in the Raman signal of adsorbed analytes.[2,5] Figure 1E shows spectra resulting from AuNP-coated LoBs in the presence (top spectrum) and absence (bottom spectrum) of 5 μM DTNB. These spectra were collected by combining SERS-active LoBs with DTNB analyte, allowing the buoyant LoBs to float to the top of a vessel, and collecting the Raman data using an 808 nm Sierra Raman spectrometer [Snowy Range Instruments LLC (SnRI)]. Figure 1C and the Figure 1E inset demonstrate the detection scheme for the LoB assay. AuNP-coated LoBs were optimized for SERS activity by starting with a known quantity of bubbles and saturating the bubble surface using progressively larger volumes of colloidal AuNPs.

Figure 2 illustrates the dynamic properties of AuNP-coated LoBs in comparison with AuNPs in a solution. For example, as the number of AuNPs (◆) in a focused laser beam was decreased, the relative error of a measurement increased sharply as a result of Brownian motion. Statistically this would be expected to follow a Poisson distribution and to increase according to $1/N^{1/2}$ as the number of nanoparticles (N) decreases. The data in Figure 2 were collected with a shot-noise-limited detector (Andor) cooled to −80 °C (SnRI New Dimension Raman microscope). Scanning electron microscopy (SEM) analysis of the particles indicated that the average size was ~50 nm, and UV−vis spectroscopy indicated a stock concentration of 6.4×10^{10} AuNPs/mL. Our probe in this study was adsorbed
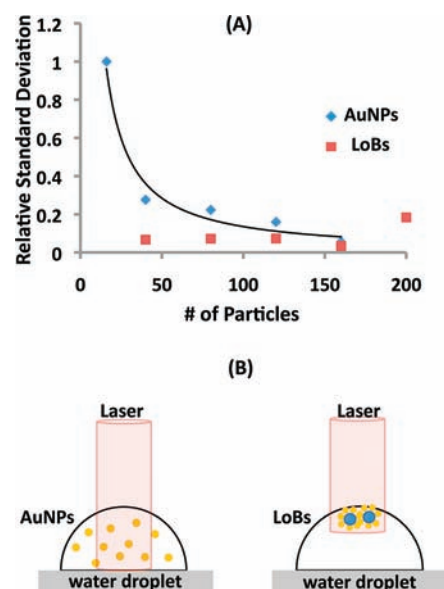

Figure 2. Increase in noise as a function of the concentration of colloidal AuNPs (blue ◆) and LoBs (red ■); the LoB concentrations were scaled by $^1/_4$ to match the AuNP values. The noise was determined by the relative standard deviation from 10 measurements. In both measurements, a focused beam was used to collect the data.

cyanide from a sodium cyanide solution at 1 ppm and pH 9. With 16 AuNPs in the focal volume of ~8 nL, the variation in the signal was 24 times that predicted for a shot-noise-limited detection system.

A goal in chemical analysis is to reduce the variation in signals in order to decrease the limit of detection (LOD), defined as LOD = $3\sigma/m$, where σ is the standard deviation and m is the slope. Our results presented in Figure 2 demonstrate the large difference in σ for the static LoBs (■) in comparison with colloidal AuNPs (◆): $\sigma = 0.05$ for 1 LoB particle compared with $\sigma = 1.0$ for 16 AuNPs in the beam. It should be noted that while the x axis in Figure 2 for AuNPs represents the change in the number of colloidal nanoparticles in the focal volume, the x axis for LoBs represents the total number of LoBs in the sample. In actuality, on the basis of their ~30 μm average diameter, the number of LoBs in the laser beam for these experiments is expected to be 1 or 2 and thus is independent of the number of LoBs in the sample (Figure 2B).

We also performed an experimental determination of the isotherm for cyanide adsorption on AuNPs and AuNP-coated LoBs. The isotherm for cyanide on AuNPs (Figure 3 top) exhibits a combination of Frumkin behavior, associated with adsorption of charged species at a charged surface, and loss of gold as a result of dissolution. The bottom panel in Figure 3 shows the isotherm we observed for cyanide on our AuNP-coated LoBs. The two isotherms have similar shapes with slightly different dependencies on the cyanide concentration.

We found the adsorption coefficient, k, to be quite different from the value of 0.16 ppb^{-1} reported by Tessier et al.[7] Our values calculated from the slope at low concentrations for AuNPs and LoBs were 0.0059 and 0.0051 ppb^{-1}, respectively. The 30-times smaller values for cyanide adsorption on our particles relative to that reported in the Tessier study may be explained by differences in surface structure and the pH difference (9 in our study vs 10 in theirs). The pK_a for HCN is 9.5, indicating that a high
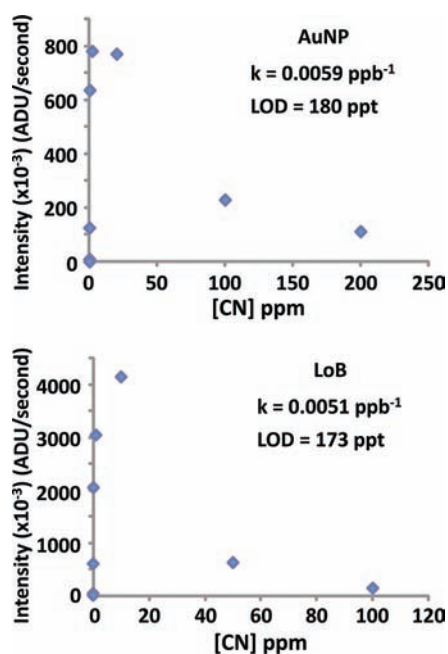
Figure 3. Cyanide adsorption isotherms for (top) colloidal AuNPs and (bottom) LoB particles. The k values were calculated from the slopes, m, between the first and second data points. The LOD was computed as $3\sigma/m$.

Figure 4. SERS spectra of cyanide and citrate on LoB (red) and AuNPs (black). These spectra indicate that citrate was not displaced by the adsorption of cyanide.

pH is required to keep the solution species as CN⁻. However, Tessier et al. reported similar k values at both low and high pH values since the adsorption process is for CN⁻. Additionally, the Au surface developed by Tessier et al. was a planar substrate with AuNP-coated polystyrene spheres. While Tessier et al. did not discuss other materials on their AuNPs, we observed strongly bound citrate that did not change intensity through our isotherm titrations.

The ζ potential of our nanoparticles prepared using the Frens protocol[6] was approximately −35 mV, indicating strongly adsorbed citrate. The strong negative charge would repel CN⁻, causing k to be lower than for a neutral surface. This may have contributed to the smaller k values we observed. The CN⁻ peak we observed was at the same location as reported elsewhere, 2125 cm⁻¹,[7−9] and the citrate peaks we observed were also located at the same wavenumbers observed by other groups.[10,11] Our spectra, shown in Figure 4, have citrate peaks at the same locations noted by Siiman et al.,[10] who also reported that the citrate was strongly adsorbed and did not change in composition or intensity over pH ranging from 2.8 to 9.9. Clearly the saturation of our surfaces did not represent 100% coverage of the surface with cyanide but rather coverage only of the fraction not covered with citrate. Thus, repulsion of CN⁻ by our citrate-coated AuNPs may be the best explanation for the difference in our observed k values relative to the study by Tessier et al.

Tessier et al. reported LOD values of 210 ppt at high pH. Our values of 180 ppt for colloidal AuNPs and 173 ppt for LoBs (Figure 3) are similar. The sharp dropoff of CN⁻ coverage at the <100 ppb solution concentration level dictates the LOD in terms of the slope. However, Figure 2A demonstrates that the σ value increases exponentially for AuNPs. To alleviate this problem, we performed the isotherm experiments using a relatively high AuNP concentration (1.8×10^9 AuNPs/mL), and we used a Raman system with a large 1 mm raster area (Sierra ORS, SnRI) to eliminate noise created by dynamic AuNP motion. The isotherm
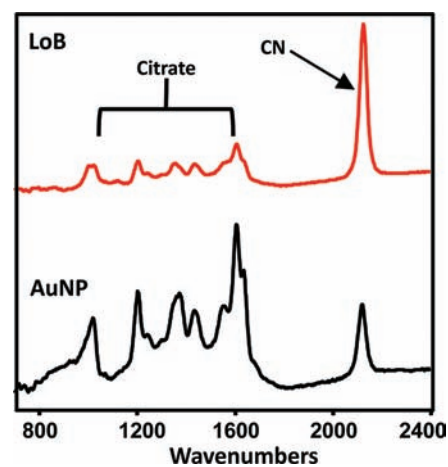
for LoBs in Figure 3 was collected with identical acquisition parameters and 1000 LoBs.

The cyanide system used in this study demonstrates LoB assays with a fairly weak reversibly binding species. An examination of the theoretical intensities predicted for colloidal AuNPs demonstrates a further advantage of the LoB assay. This can be seen from the following equation:

$$I = F\theta N$$

where I (photons/s) describes the SERS intensity from an analyte from an AuNP colloid with a fractional analyte coverage of θ and N nanoparticles/mL. F is a factor that converts coverage into Raman intensity. Assuming a Langmuir isotherm and solving this equation for I as a function of the number of nanoparticles provides a model that provides a better understanding of AuNP SERS assays. Of particular interest are the cases when the analyte concentration c_0 is low and the adsorption coefficient, k, is large. In this case, θ is no longer dictated by c_0, as the amount of material adsorbed onto the surface becomes a significant fraction of the total amount of analyte in the solution. We solved for I as a function of c_0 and produced an equation to calculate the effect of analyte depletion by the AuNPs.

Figure 5 illustrates the interplay between k and θ as a function of the number of particles present. It can be seen that as the concentration of nanoparticles decreases, the coverage increases, and as k increases, the coverage increases. Intuitively this result is not surprising, but since σ increases with fewer colloidal AuNPs, this result dramatically illustrates the difficulty of colloidal AuNP assays. For example, the data for AuNPs in Figure 2A begins at 3.2×10^6 AuNPs/mL and already shows significant fluctuations due to dynamic motion into and out of the laser beam. This is not expected to occur with LoBs, as evidenced by the relatively constant σ(LoB) observed (Figure 2A). The simple model in Figure 5 predicts that a fundamental limitation occurs as noise increases while surface coverage increases. Although this may not be observed in a colloidal AuNP system at fairly high concentrations, it is the fundamental limit of a system examining trace levels of materials.

To demonstrate the value of LoBs with a neutral adsorbate and a high k value, we chose the popular tag DTNB. Grubisha et al.[12] reported femtomolar detection of prostate-specific antigen with
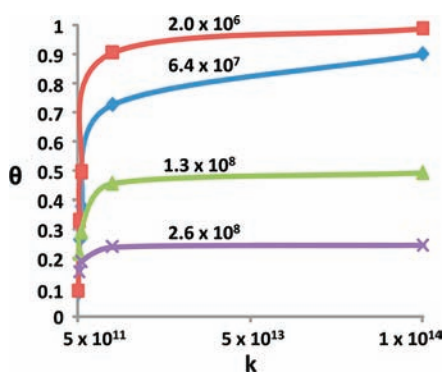
Figure 5. An illustration of the theoretical coverage vs k. The curves relate to the theoretical concentration of nanoparticles in a given sample.
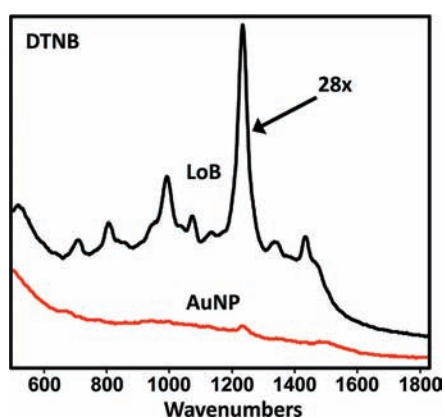

Figure 6. Representative SERS spectra of DTNB at equal concentration on a mass-equivalent amount of 50 nm AuNPs. The LoB-bound AuNPs did not aggregate and fall out of solution. The colloidal AuNP particles did aggregate, and their signal was lost.

the succinimide derivative of DTNB. Specifically, they used immobilized particles on a glass slide to avoid aggregation effects from AuNPs in solution, and their ultimate detection limit was detected hypothetically by looking at a ratio of the 22 μm laser beam spot and the 5 mm spot of immobilized AuNPs used in the study. Our experiment with DTNB consisted of a comparison of colloidal AuNPs and LoBs. Figure 6 illustrates the signal difference from LoBs and colloidal AuNPs under conditions with an equivalent amount of AuNPs in both analyses. At 5 μM DTNB, we observed a signal 28 times larger on the LoB than on the colloidal AuNPs. We also did not observe citrate at this concentration, as it was displaced from the AuNP surface by the strongly binding DTNB. This difference can be easily understood from the study by Pierre et al.[2] using 2-naphthalenethiol (2-NT). In their study with 2-NT, Pierre et al. found that displacement of the citrate by the strong thiol adsorption led to a time-dependent change in signal due to aggregation. A SERS-active LoB has a stable aggregated surface of AuNPs and through agitation has the ability to interrogate the solution for DTNB. The colloidal AuNPs are stable when citrate is strongly adsorbed but rapidly aggregate and fall out of solution as DTNB is adsorbed and the AuNP surface charge is neutralized.

The number of LoBs observed in our DTNB experiment is 1. Our 25 μm laser beam is smaller than a single LoB. We used 200 LoBs in our experiment and made two observations: (1) we

could translate across the surface of our droplet and see signal variations indicating that we were detecting individual LoBs, and (2) we examined the droplet with a light microscope and found that our 200 LoBs were uniformly distributed in a monolayer. The localization of our LoB particles at the top of a droplet is equivalent to the creation of a pellet by a paramagnetic pull-down. The ability to mix large volumes of samples with a small number of LoBs that localize rapidly through their buoyant force could be advantageous over the paramagnetic counterpart, which requires an external magnetic force that decays rapidly with the distance from the magnet. Furthermore, the available chemistries for Au surface modification present many opportunities for the LoB concept in sensing applications.

■ ASSOCIATED CONTENT

Ⓢ Supporting Information. General protocol for the preparation of SERS-active AuNP-coated glass bubbles and details regarding LoB enumeration and instrumentation used for the LoB assays. This material is available free of charge via the Internet at http://pubs.acs.org.

■ AUTHOR INFORMATION

Corresponding Author
carron@uwyo.edu

■ REFERENCES

(1) Mallouk, T. E.; Sen, A. *Sci. Am.* **2009**, *300*, 72.
(2) Pierre, M. C.; Mackie, P.; Roca, M.; Haes, A. *J. Phys. Chem. C* **2011**, *115*, 18511.
(3) Freeman, R. G.; Grabar, K. C.; Allison, K. J.; Bright, R. M.; Davis, J. A.; Guthrie, A. P.; Hommer, M. B.; Jackson, M. A.; Smith, P. C.; Walter, D. G.; Natan, M. J. *Science* **1995**, *267*, 1629.
(4) Karrasch, S.; Dolder, M.; Schabert, F.; Ramsden, J.; Engel, A. *Biophys. J.* **1993**, *65*, 2437.
(5) Wang, H.; Levin, C. S.; Halas, N. *J. Am. Chem. Soc.* **2005**, *127*, 14992.
(6) Frens, G. *Nature* **1973**, *241*, 20.
(7) Tessier, P. M.; Christesen, S. D.; Ong, K. K.; Clemente, E. M.; Lenhoff, A. M.; Kaler, E. W.; Velev, O. D. *Appl. Spectrosc.* **2002**, *56*, 1524.
(8) Shelton, R. D.; Haas, J. W., III; Wachter, E. A. *Appl. Spectrosc.* **1994**, *48*, 1007.
(9) Premasiri, W. R.; Clarke, R. H.; Londhe, S.; Womble, M. E. *J. Raman Spectrosc.* **2001**, *32*, 919.
(10) Siiman, O.; Bumm, L. A.; Callaghan, R.; Blatchford, C. G.; Kerker, M. *J. Phys. Chem.* **1983**, *89*, 1014.
(11) Kerker, M.; Siiman, O.; Bumm, L. A.; Wang, D. S. *Appl. Opt.* **1980**, *19*, 3253.
(12) Grubisha, D. S.; Lipert, R. J.; Park, H.-Y.; Driskell, J.; Porter, M. D. *Anal. Chem.* **2003**, *75*, 5936.